Epithelial *Bmpr1a* regulates differentiation and proliferation in postnatal hair follicles and is essential for tooth development

Thomas Andl[1], Kyung Ahn[3], Alladin Kairo[1], Emily Y. Chu[1], Lara Wine-Lee[3], Seshamma T. Reddy[1], Nirvana J. Croft[1], Judith A. Cebra-Thomas[1], Daniel Metzger[4], Pierre Chambon[4], Karen M. Lyons[5], Yuji Mishina[6], John T. Seykora[1], E. Bryan Crenshaw III[3] and Sarah E. Millar[1,2,*]

[1]Department of Dermatology, University of Pennsylvania Medical School, Philadelphia, PA 19104, USA
[2]Department of Cell and Developmental Biology, University of Pennsylvania Medical School, Philadelphia, PA 19104, USA
[3]Center for Childhood Communication, Abramson Research Center, The Children's Hospital of Philadelphia, Philadelphia, PA 19104, USA
[4]Institut de Génétique et de Biologie Moléculaire et Cellulaire, CNRS/INSERM/ULP, Collège de France, BP 163, 67404 Illkirch Cedex, France
[5]Departments of Molecular, Cell and Developmental Biology, Orthopaedic Surgery, and Biological Chemistry, David Geffen School of Medicine at UCLA, Los Angeles, CA 90095, USA
[6]Laboratory of Reproductive and Developmental Toxicology, National Institute of Environmental Health Sciences, Research Triangle Park, NC 27709, USA
*Author for correspondence (e-mail: millars@mail.med.upenn.edu)

Accepted 5 February 2004

Development 131, 2257-2268
Published by The Company of Biologists 2004
doi:10.1242/dev.01125

Summary

Bone morphogenetic protein (BMP) signaling is thought to perform multiple functions in the regulation of skin appendage morphogenesis and the postnatal growth of hair follicles. However, definitive genetic evidence for these roles has been lacking. Here, we show that Cre-mediated mutation of the gene encoding BMP receptor 1A in the surface epithelium and its derivatives causes arrest of tooth morphogenesis and lack of external hair. The hair shaft and hair follicle inner root sheath (IRS) fail to differentiate, and expression of the known transcriptional regulators of follicular differentiation *Msx1, Msx2, Foxn1* and *Gata3* is markedly downregulated or absent in mutant follicles. *Lef1* expression is maintained, but nuclear β-catenin is absent from the epithelium of severely affected mutant follicles, indicating that activation of the WNT pathway lies downstream of BMPR1A signaling in postnatal follicles. Mutant hair follicles fail to undergo programmed regression, and instead continue to proliferate, producing follicular cysts and matricomas. These results provide definitive genetic evidence that epithelial *Bmpr1a* is required for completion of tooth morphogenesis, and regulates terminal differentiation and proliferation in postnatal hair follicles.

Key words: Hair follicle, Skin, Tooth, BMP, BMPR1A, BMPR1B, β-catenin, *Gata3*, *Msx*, *Foxn1*

Introduction

Postnatal hair growth relies on a precise balance between proliferation and differentiation of follicular epithelial cells. The base of the hair follicle contains relatively undifferentiated, pluripotent epithelial matrix cells that proliferate rapidly during periods of hair growth (anagen). The matrix is derived from long-lived epithelial stem cells located in the permanent, bulge region of the follicle (Cotsarelis et al., 1990; Oshima et al., 2001; Taylor et al., 2000). The stem cells proliferate transiently at anagen onset and otherwise remain quiescent (Wilson et al., 1994). The matrix gives rise to several different hair follicle lineages: the medulla, cortex and cuticle of the hair shaft; and the cuticle, Huxley's layer and Henle's layer of the IRS (Oshima et al., 2001).

Periods of hair growth are followed by a regression phase (catagen), when proliferation and differentiation of follicular epithelial cells cease and the lower two-thirds of the follicular epithelium degenerates (Lindner et al., 1997). Following catagen the follicles enter a quiescent phase (telogen). The onset of a new anagen phase is thought to involve signaling between the dermal component of the hair follicle, the dermal papilla and epithelial cells (Cotsarelis et al., 1990; Oliver and Jahoda, 1988).

Intercellular communication between the dermis and surface epithelium, and within the surface epithelium, is also crucial for the embryonic morphogenesis of hair follicles and other epithelial appendages, such as teeth and mammary glands, and several classes of secreted signaling molecules are implicated at early stages of appendage development (reviewed by Hardy, 1992; Jernvall and Thesleff, 2000; Millar, 2002; Veltmaat et al., 2003). Among these are BMPs, which function by binding type 1 (BMPR1A and BMPR1B) and type 2 (BMPR2) transmembrane serine/threonine kinase receptors, resulting in phosphorylation of the intracellular proteins SMADs 1, 5 and 8. Phosphorylated SMADs bind to SMAD4 and translocate to the nucleus, where they complex with transcription factors and regulate target gene transcription (Mishina, 2003). Ectopic expression experiments and analysis of mice lacking the BMP inhibitor noggin suggest that BMP signals act during embryogenesis to retard hair follicle development, and may

control the spacing of hair and feather follicles (Botchkarev et al., 1999; Jung et al., 1998; Noramly and Morgan, 1998). Postnatally, ectopic expression studies suggest that BMP inhibition controls anagen onset (Botchkarev et al., 2001), and that BMP signaling regulates hair-shaft differentiation (Kulessa et al., 2000). Existing evidence suggests that BMPs play crucial roles at multiple stages of tooth morphogenesis (Jernvall and Thesleff, 2000), and BMP mRNAs are also expressed in developing mammary glands (Phippard et al., 1996).

Despite abundant data suggesting key roles for BMP signals in appendage development and in postnatal hair follicle differentiation and cycling, definitive genetic evidence from loss-of-function mutations in BMP or BMP receptor genes is lacking because of the early lethality of most of these mutants (Mishina, 2003). As the BMPR1A receptor is broadly expressed in the epidermis and hair follicles (Botchkarev, 2003), we investigated the requirement for epithelial *Bmpr1a* in these processes using several different mouse lines that express Cre recombinase (Lewandoski, 2001) in epidermal cells and their derivatives, in combination with a conditional allele of *Bmpr1a* (Ahn et al., 2001; Mishina et al., 2002). Tooth morphogenesis was arrested in the most severely affected conditional mutant mice, and postnatal development of hair follicles was strikingly defective. Hair follicle matrix cells failed to differentiate towards hair shaft or IRS, and expression of several known transcriptional regulators of hair shaft and IRS differentiation was decreased or absent. Mutant follicles failed to undergo catagen, instead continuing to proliferate to produce matricomas and follicular cysts. These results demonstrate that epithelial *Bmpr1a* plays essential roles in controlling differentiation and proliferation in postnatal hair follicles, as well as being required for completion of tooth morphogenesis.

Materials and methods

Generation and breeding of mouse lines, tamoxifen treatment and detection of floxed and recombined alleles

A *K14-Cre* transgene was made by inserting a modified *Cre* cDNA fragment PCR-amplified from the pACN vector (Bunting et al., 1999) into the *Bam*HI site of a K14 expression vector (Andl et al., 2002). The transgene was microinjected into fertilized eggs from a B6SJLF1/J×B6SJLF1/J cross (Jackson Laboratories). Transgenic founders were tested for Cre activity by breeding to *ROSA26R* mice (B6.129S4-*Gt(ROSA)26Sor*^{tm1Sor}) (Soriano, 1999) (Jackson Laboratories). Detection of β-galactosidase in embryo wholemounts and 20 μm frozen sections of P1 tissue were as described previously (Phippard et al., 1999; Wang et al., 1997).

Mice homozygous for a floxed allele of *Bmpr1a* (*Bmpr1a*$^{floxP\text{-}neo}$) (Ahn et al., 2001; Mishina et al., 2002), referred to here as *Bmpr1a*^{cl}, were crossed to *K14-Cre* or *K14-Cre-ER*^{T2} (Indra et al., 2000) transgenic mice, and progeny heterozygous for both *K14-Cre* or *K14-Cre-ER*^{T2} and *Bmpr1a*^{cl} were crossed to *Bmpr1a*^{cl} homozygotes. *Brn4-Cre* line *bcre-32* transgenic mice (Ahn et al., 2001) were used in combination with *Bmpr1a*^{cl} and heterozygous *Bmpr1a* null (*Bmpr1a*^{null}) (Mishina et al., 1995) mice. *Bmpr1a*$^{null/+}$ males homozygous for *bcre-32* were crossed with females of genotype *Bmpr1a*$^{cl/cl}$. In addition, we used mice carrying a null allele of *Bmpr1b* (*Bmpr1b*^{null}) (Yi et al., 2001): *Bmpr1a*$^{null/+}$; *Bmpr1b*$^{null/+}$ males homozygous for *bcre-32* were crossed with *Bmpr1a*$^{cl/cl}$; *Bmpr1b*$^{null/+}$ females. PCR detection of wild-type, floxed and recombined *Bmpr1a* alleles was as described previously (Mishina et al., 2002). Newborn epidermis was isolated mechanically after incubation of skin overnight in 0.25% trypsin in PBS at 4°C. For tamoxifen induction, dorsal hair (if present) was clipped and 0.5 mg tamoxifen (Sigma) in 100 μl ethanol was applied to dorsal skin three times at 48 hour intervals. Controls were treated with vehicle only.

Histology, follicle density measurements, immunofluorescence, BrdU incorporation, TUNEL assays and in situ hybridization

Tissue samples were fixed in 4% paraformaldehyde, paraffin embedded and sectioned at 5 μm. Samples containing bone were decalcified with 4% formic acid, 4% hydrochloric acid for 4 hours after fixation. For histological analysis, sections were stained with Hematoxylin and Eosin. For hair follicle density measurements, 2-4 control animals and 2-4 experimental animals were used for each developmental stage. Follicles were counted at 10× magnification in 10 microscopic fields for each sample. Statistical significance was calculated using a two-tailed Student's *t*-test.

Alkaline phosphatase staining for identification of dermal papillae was as described previously (Handjiski et al., 1994). For immunofluorescence staining, sections were microwave pretreated and incubated with primary antibodies against phospho-SMAD1, phospho-SMAD5 and phospho-SMAD8 (polyclonal rabbit serum, Cell Signaling Technology; 1:50), type I hair keratin (mouse monoclonal antibody clone AE13) (Lynch et al., 1986) (1:10), trichohyalin (mouse monoclonal antibody clone AE15; 1:6) (O'Guin et al., 1992), mouse keratin 6 (polyclonal rabbit serum, Covance; 1:300), GATA3 (mouse monoclonal antibody, Santa Cruz HCG3-31; 1:100) and cytokeratin K17 (polyclonal rabbit serum; 1:500) (McGowan and Coulombe, 1998). For detection of nuclear β-catenin, antibody clone 15B8 (Sigma; 1:1000) was used in combination with the MOM kit (Vector Laboratories). Polyclonal rabbit serum (ten Dijke et al., 1994) (1:100) was used for detection of BMPR1A in 8 μm cryosections. Sections were counterstained with 2 μg/ml Hoechst 33258 (Sigma).

For proliferation assays, mice were injected with BrdU (50 μg BrdU/g body weight) and sacrificed after 1 hour. Detection of BrdU incorporation with anti-BrdU antibody (Roche) was as previously described (Andl et al., 2002). The In Situ Cell Death Detection Kit (Roche Diagnostics) was used for apoptosis assays.

In situ hybridization with ^{35}S-labeled probes, and whole-mount and paraffin section in situ hybridization with digoxigenin-labeled probes were as described previously (Decimo et al., 1995; Grachtchouk et al., 2003; Reddy et al., 2001). The following PCR products containing a T7 promoter were used as templates for sense and antisense probe synthesis: *Foxn1* (Accession Number NM_008238, nucleotides 1720-2339), and *Cre* (Accession Number AF169416, nucleotides 2533-3151). *Msx*, *Lef1*, *Wnt10b* and *Shh* probes were as described previously (Andl et al., 2002; Jowett et al., 1993).

Results

BMP signaling is active in postnatal hair follicles

Cells responding to BMP signals can be identified by the presence of phosphorylated SMAD1, SMAD5 and SMAD8 in the nucleus (von Bubnoff and Cho, 2001). To determine the sites of BMP signaling activity in postnatal hair follicles, we used an antibody to phospho-SMAD1/5/8 at different stages of the embryonic and first postnatal hair growth cycles. In early anagen [postnatal day (P) 5], nuclear phospho-SMAD was detected in the companion layer of the outer root sheath (Fig. 1A,B). By full anagen (P13), phospho-SMAD staining was present in precursor cells of the medulla, cortex and cuticle of the hair shaft, in a subset of IRS cells, and in the companion layer (Fig. 1C,D). Phospho-SMAD staining faded at the

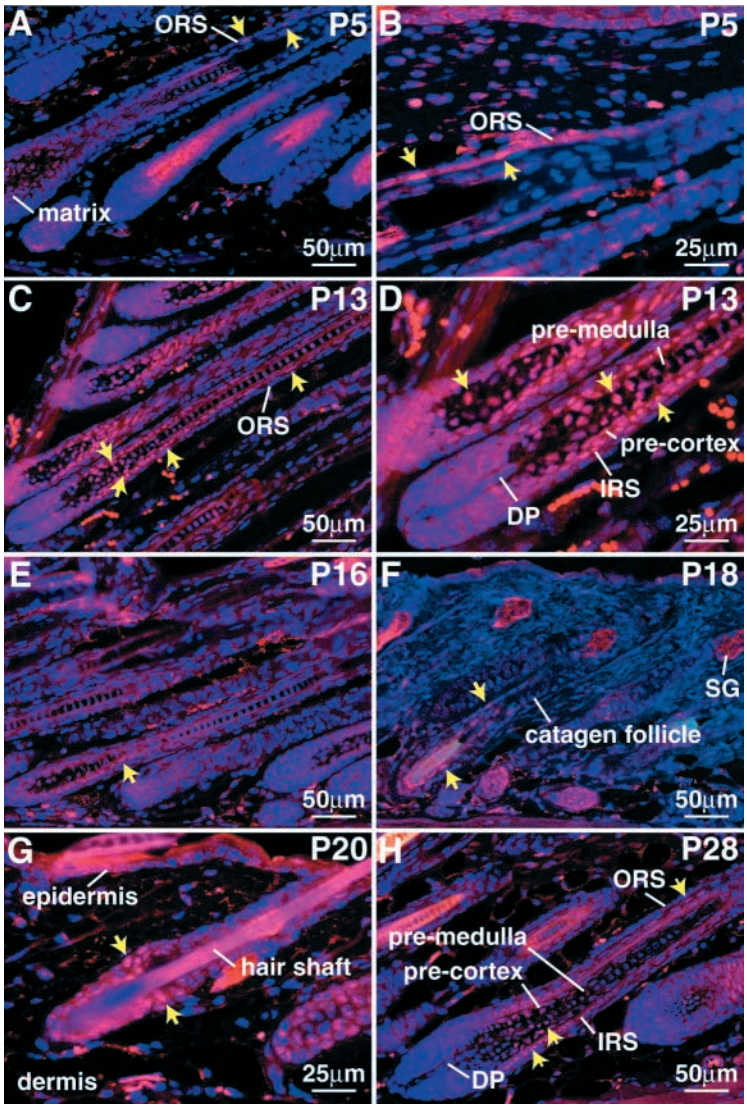

Fig. 1. Anti-phospho-SMAD1/5/8 immunofluorescence (red) of paraffin sectioned mid-dorsal skin at P5 (early anagen; A,B), P13 (full anagen; C,D), P16 (anagen-catagen transition; E), P18 (catagen; F), P20 (telogen; G) and P28 (first postnatal anagen; H). Nuclei are counterstained with Hoechst 33258 and appear blue. Presence of nuclear phospho-SMAD is indicated by yellow arrows. (B,D) Higher magnification photographs of the follicles shown in A and C, respectively. Diffuse red staining in the center of some follicles is due to autofluorescence of the hair shaft. ORS, outer root sheath; IRS, inner root sheath; DP, dermal papilla; SG, sebaceous gland.

anagen-catagen transition (P16; Fig. 1E) and during catagen was weakly present in the companion layer and around the forming club hair (P18; Fig. 1F). During telogen (P20), staining for nuclear phospho-SMAD was present in cells of the bulge, the region where stem cells are located (Fig. 1G). Phospho-SMAD staining patterns during the first postnatal hair cycle, beginning at approximately P23, were similar to those in the embryonic hair cycle (Fig. 1H and data not shown). We did not observe nuclear phospho-SMAD in the dermal papilla, possibly due to expression of noggin in dermal papilla cells (Kulessa et al., 2000).

Generation of mice lacking *Bmpr1a* in the epidermis and its derivatives

Bmpr1a-deficient mice die early in gestation (Mishina et al., 1995). To determine the requirement for *Bmpr1a* in development of the epidermis and its appendages, we generated three lines of transgenic mice that constitutively express Cre recombinase in epidermal cells under the control of a well-characterized keratin 14 (*K14*) promoter (Wang et al., 1997). This promoter is active in surface ectoderm and basal epidermis from embryonic day (E) 9.5, and drives expression in developing hair follicle and tooth epithelia (Byrne et al., 1994; Dassule et al., 2000). In addition, we made use of *bcre-32* mice that carry a *Brn4-Cre* transgene that directs *Cre* expression to the neural tube, and also shows ectopic *Cre* expression in limb epithelium and in ventral epidermis (Ahn et al., 2001). Lastly we used tamoxifen-inducible *K14-Cre-ER^{T2}* mice, which express a Cre recombinase-estrogen receptor fusion protein under the control of the *K14* promoter (Indra et al., 2000). The *K14-Cre* and *bcre-32* transgenics were crossed to a *ROSA26R* reporter strain that carries a *lacZ* gene whose expression is activated by Cre-mediated excision of an inhibitory sequence, allowing identification of cells that express Cre and their descendents by staining for β-galactosidase (Soriano, 1999). β-galactosidase expression in *K14-Cre* mice was assayed at E14.5 and P1, and was observed specifically in epidermis, hair follicles, oral epithelium and developing teeth, with very low levels in the esophagus and forestomach, as previously described (Byrne et al., 1994; Vassar and Fuchs, 1991; Vassar et al., 1989; Wang et al., 1997) (Fig. 2A-C and data not shown). β-galactosidase activity in the suprabasal epidermis and in all hair follicle epithelial cells reflects derivation of these cells from basal epidermis and *K14*-expressing follicular stem cells, and inheritance of the recombined *ROSA26R* allele (Vasioukhin et al., 1999). All three lines showed similar Cre activity at this level of analysis. Strong Cre activity was observed in ventral epidermis of *bcre-32* embryos by E15 (Fig. 2D).

Each of the *Cre*-expressing lines was mated to mice carrying a conditional allele of *Bmpr1a*, *Bmpr1a^{cl}*, in which exon 2 of the *Bmpr1a* gene is flanked by *loxP* sites (Ahn et al., 2001; Mishina et al., 2002). Mice homozygous for *Bmpr1a^{cl}* show no apparent phenotype (Ahn et al., 2001; Mishina et al., 2002). However, global expression of Cre recombinase in *Bmpr1a^{cl}* homozygotes produces a phenotype identical to the null mutant phenotype, indicating that deletion of exon 2 produces a null allele (Mishina et al., 2002).

Bmpr1a^{cl} heterozygotes carrying *Cre* transgenes, and *Bmpr1a$^{cl/cl}$* mice lacking a *Cre* transgene, were indistinguishable from non-transgenic mice that were wild type for *Bmpr1a*. *Bmpr1a^{cl}* homozygotes carrying *K14-Cre* transgenes displayed phenotypes of graded severity depending on the *Cre* line used. This observation suggested subtle differences in the level of activity of Cre recombinase in the three lines, as all of the mice were maintained on a similar,

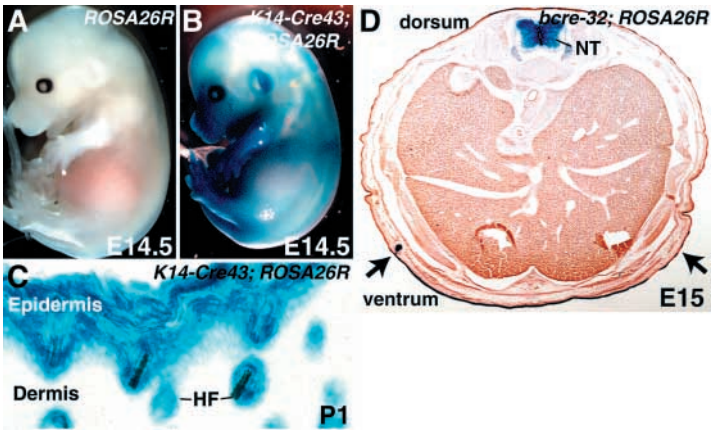

Fig. 2. Activity of Cre recombinase in *Cre* transgenic lines revealed by X-gal staining. (A,B) Wholemounts of E14.5 *ROSA26R* (A) and *K14-Cre43*; *ROSA26R* (B) embryos. Cre activity is detected globally in the epidermis of the *K14-Cre43* embryo. (C) Frozen section of *K14-Cre43*; *ROSA26R* dorsal skin at P1. (D) Transverse section of E15 *bcre-32*; *ROSA26R* embryo torso after whole-mount X-gal staining. Arrows mark the limits of staining in ventral epidermis. HF, hair follicle; NT, neural tube.

mixed strain background. *K14-Cre43*; *Bmpr1a*$^{cl/cl}$ mice died within 24 hours of birth, and displayed severe limb defects and open eyes (Fig. 3A). The limb defects reflected the known requirement of epithelial *Bmpr1a* for maintenance of the apical ectodermal ridge (Ahn et al., 2001). *K14-Cre52*; *Bmpr1a*$^{cl/cl}$ mice usually died by P4. They had grossly normal limbs and eyes, were severely runted, and lacked external hair and teeth (Fig. 3C,D,E). *K14-Cre40*; *Bmpr1a*$^{cl/cl}$ mice showed the weakest phenotype of the constitutive *K14-Cre* lines and occasionally survived for several months. These mice were runted, and showed greatly decreased external hair (Fig. 3F-H). *K14-Cre-ER*^{T2}; *Bmpr1a*$^{cl/cl}$ mice that had not been treated with tamoxifen survived for at least 6 months. They displayed a sparse hair phenotype that became more severe with age (Fig. 3I). Surviving *K14-Cre40*; *Bmpr1a*$^{cl/cl}$ and *K14-Cre-ER*^{T2}; *Bmpr1a*$^{cl/cl}$ mice had abnormal growths under their nails (Fig. 3J). Topical tamoxifen treatment of *K14-Cre-ER*^{T2}; *Bmpr1a*$^{cl/cl}$ mice caused these animals to become sickly, requiring euthanasia 7 days after cessation of treatment. This may have been due to trans-cutaneous absorption of tamoxifen and induction of *Bmpr1a*^{cl} recombination in internal stratified epithelia. Homozygous *bcre-32* transgenic mice that were also heterozygous for a null allele of *Bmpr1a* (*Bmpr1a*^{null}) (Mishina et al., 1995) were crossed to *Bmpr1a*$^{cl/cl}$ mice to produce progeny of genotype *bcre-32*; *Bmpr1a*$^{cl/null}$, as well as *bcre-32*; *Bmpr1a*$^{cl/+}$ controls. *bcre-32*; *Bmpr1a*$^{cl/null}$ mice survived for up to 17 days and showed absence of external hair in the mid-ventrum, corresponding to the region of Cre activity in ventral epidermis (Fig. 3B). The lethality of *bcre-32*; *Bmpr1a*$^{cl/null}$ mice was due to hydrocephalus and CNS defects (data not shown). *K14-Cre43*; *Bmpr1a*$^{cl/cl}$ and *K14-Cre52*; *Bmpr1a*$^{cl/cl}$ mice had oral abnormalities, resulting from defective tooth development (see below), and had difficulty suckling. Decreased lifespan of *K14-Cre40*; *Bmpr1a*$^{cl/cl}$ mice may have been due to loss of *Bmpr1a* in internal epithelia.

Absence of BMPR1A protein from *K14-Cre43*; *Bmpr1a*$^{cl/cl}$ newborn epidermis and hair follicle epithelium was confirmed by immunofluorescence with anti-BMPR1A antibody (Fig. 3K,L). In addition, PCR of genomic DNA, using primers specific for the floxed, recombined and wild-type alleles (Mishina et al., 2002), demonstrated that the *Bmpr1a*^{cl} allele was efficiently recombined in the epidermis of *K14-Cre43*; *Bmpr1a*$^{cl/cl}$ mice to produce a non-functional allele (Mishina et al., 2002) (Fig. 3M). Skin-specific recombination of the *Bmpr1a*^{cl} allele in uninduced *K14-Cre-ER*^{T2}; *Bmpr1a*$^{cl/cl}$ mice was demonstrated by PCR of genomic DNA extracted from skin and other organs (Fig. 3M). This result indicated that Cre-ER^{T2} is active at a low level in the epidermis of *K14-Cre-ER*^{T2} mice, even in the absence of tamoxifen. Leakiness of Cre-ER^{T2} activity was not observed in previous studies (Indra et al., 2000; Li et al., 2000), and may have been detected because of the strain background on which our mice were maintained, or because of particular susceptibility of the *Bmpr1a*^{cl} locus to recombination at even very low levels of Cre activity.

Accelerated hair follicle morphogenesis in epithelial *Bmpr1a* mutants

Development of primary hair follicles in mouse embryos is initiated at approximately E14, and secondary hair follicles develop in several waves between approximately E16 and birth. To determine whether deletion of epithelial *Bmpr1a* affects hair follicle morphogenesis, we examined the histology of *K14-Cre*; *Bmpr1a*$^{cl/cl}$ dorsal and ventral skin, and *bcre-32*; *Bmpr1a*$^{cl/null}$ mid-ventral skin, between E16.5 and birth. In addition, anti-K17 antibody was used to clearly reveal the location of developing hair follicles (Fig. 4C,D). For all the mutants analyzed, newborn skin appeared similar to littermate controls (Fig. 4E-H and data not shown). Measurements of follicle density in newborn dorsal *K14-Cre43*; *Bmpr1a*$^{cl/cl}$ and littermate control skin revealed no significant difference (average of 12±3 versus 12±2 follicles per mm; P=0.766). At E16.5 and later embryonic stages, mutant follicles were histologically similar to controls (Fig. 4A,B and data not shown). However, we found that the follicle density in E16.5 *K14-Cre43*; *Bmpr1a*$^{cl/cl}$ dorsal skin was significantly greater than in control dorsal skin (7±2 versus 5±2 follicles per mm; P=0.0002). As the sizes of mutant and control individuals were similar at these stages, these results suggested that follicular morphogenesis was accelerated in *Bmpr1a* mutants, but that the total number of follicles that developed by birth was not affected by loss of epithelial *Bmpr1a*.

To determine whether *Bmpr1a* might act redundantly with *Bmpr1b* in hair follicle patterning, we examined the mid-ventral skin of *bcre-32*; *Bmpr1a*$^{cl/null}$ mice that were also homozygous for a targeted deletion of *Bmpr1b* (*Bmpr1b*^{null}) (Yi et al., 2000) at E17.5. At this stage the histology and follicle density of *bcre-32*; *Bmpr1a*$^{cl/null}$; *Bmpr1b*$^{null/null}$ ventral skin was indistinguishable from *bcre-32*; *Bmpr1a*$^{cl/null}$ ventral skin; however, the average follicle density was significantly greater than in control littermate ventral skin (2±1 versus 1±1 per mm; P=0.0074). At birth, ventral skin from *bcre-32*; *Bmpr1a*$^{cl/null}$; *Bmpr1b*$^{null/null}$, *bcre-32*; *Bmpr1a*$^{cl/null}$ and control mice had a similar histology, and follicle densities did not differ

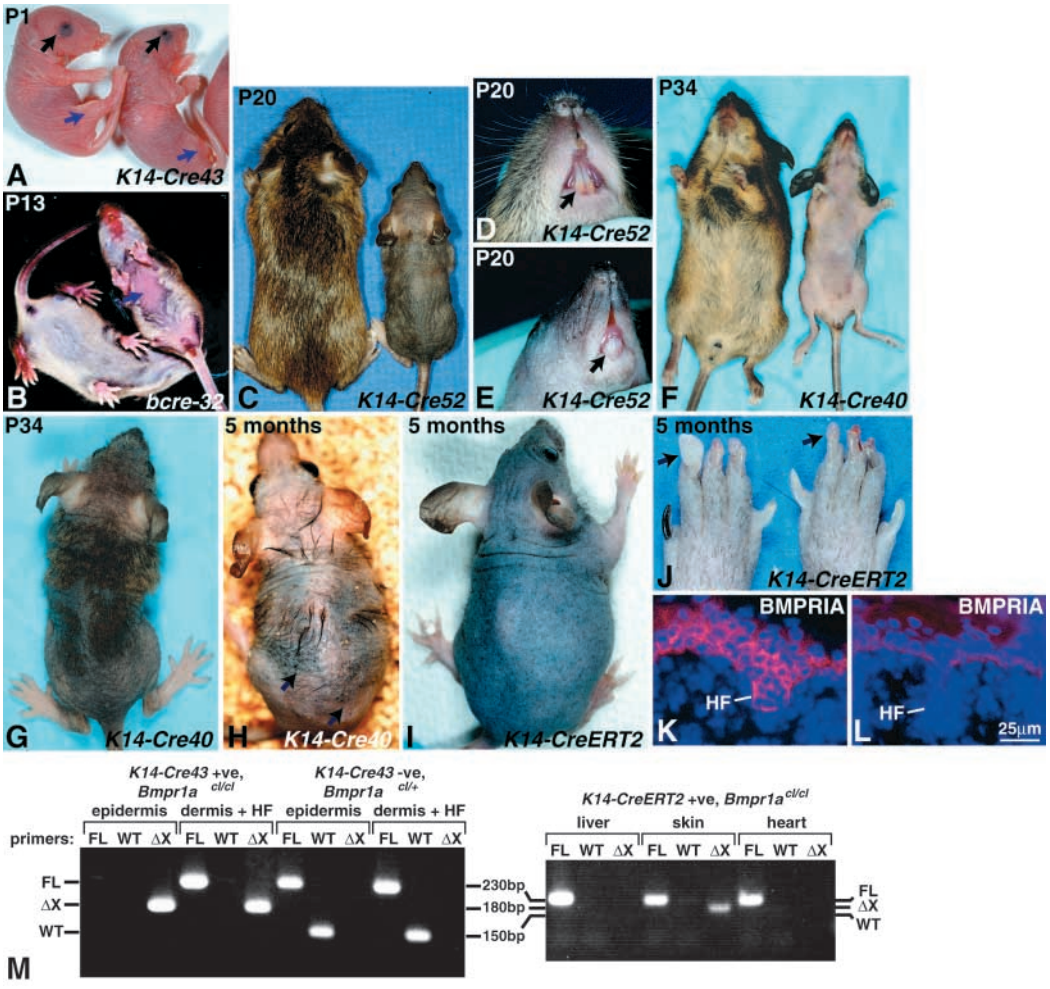

Fig. 3. Phenotypes of mice carrying epidermal-specific deletions of *Bmpr1a*. (A) *K14-Cre43*; *Bmpr1a*$^{cl/cl}$ (right) and *K14-Cre43*; *Bmpr1a*$^{cl/+}$ control (left) newborns. The homozygous mutant lacks hindlimbs (blue arrow) and has open eyes (black arrow). (B) Ventral view of P13 *bcre-32*; *Bmpr1a*$^{cl/null}$ (right) and *bcre-32*; *Bmpr1a*$^{cl/+}$ (left) littermates. The mutant lacks mid-ventral hair (arrow). (C) P20 *K14-Cre52;* *Bmpr1a*$^{cl/cl}$ (right) and *K14-Cre52*; *Bmpr1a*$^{cl/+}$ (left) littermates. (D,E) Absence of incisor teeth (arrows) in a *K14-Cre52*; *Bmpr1a*$^{cl/cl}$ mouse at P20 (E), compared with a heterozygous littermate control (D). (F) *K14-Cre40*; *Bmpr1a*$^{cl/cl}$ (right) and *K14-Cre40*; *Bmpr1a*$^{cl/+}$ (left) littermates at P34. (G) *K14-Cre40*; *Bmpr1a*$^{cl/cl}$ mouse at P34. (H) *K14-Cre40*; *Bmpr1a*$^{cl/cl}$ mouse at 5 months. Arrows indicate pigment accumulations. (I) Uninduced *K14-Cre-ER*^{T2}; *Bmpr1a*$^{cl/cl}$ mouse at 5 months. (J) Front paws from uninduced 5-month-old *K14-Cre-ER*^{T2}; *Bmpr1a*$^{cl/cl}$ mouse showing growths under the nails (arrows). (K,L) Anti-BMPR1A immunofluorescence (red) of newborn *K14-Cre43*; *Bmpr1a*$^{cl/+}$ control (K) and *K14-Cre43*; *Bmpr1a*$^{cl/cl}$ (L) skin cryosections. BMPR1A is present in control epidermis and hair follicle (HF), but only background basal lamina staining is detected in mutant skin. Nuclei are counterstained with Hoechst 33258. (M) Left side: PCR amplification of genomic DNA from epidermis, and dermis containing HF germs, from a newborn *K14-Cre43*; *Bmpr1a*$^{cl/cl}$ mouse and a *Bmpr*$^{cl/+}$ littermate control. Primers detect the unrecombined floxed (FL), wild-type (WT) and recombined (lacking exon 2; ΔX) alleles, and produce amplification products of 230 bp, 150 bp and 180 bp, respectively. Right side: PCR amplification of genomic DNA from organs of a 5-month-old uninduced *K14-Cre-ER*^{T2}; *Bmpr1a*$^{cl/cl}$ mouse using the same primers.

significantly (Fig. 4G-I). These data provide further evidence for accelerated follicular morphogenesis in *Bmpr1a* mutants, and indicate that epithelial *Bmpr1a* and *Bmpr1b* do not act redundantly in embryonic hair follicle development.

Tooth development is arrested in epithelial *Bmpr1a* mutants

Surviving *K14-Cre*; *Bmpr1a*$^{cl/cl}$ adult females were able to nurse pups, indicating that functional mammary glands developed. Histological analysis revealed that mammary buds and glands were present in severely affected *K14-Cre*; *Bmpr1a*$^{cl/cl}$ females at E13.5 and birth, respectively, and whole-mount in situ hybridization with a probe for the mammary bud marker *Wnt10b* revealed a normal pattern of bud development at E13.5 (Fig. 4J-O). However, determining whether these mutants have subtle defects in mammary morphogenesis will require further analysis.

By contrast, tooth development was strikingly affected in *K14-Cre*; *Bmpr1a*$^{cl/cl}$ mice. Analysis of the histology of the oral cavity of *K14-Cre43*; *Bmpr1a*$^{cl/cl}$ newborns revealed a complete absence of incisor or molar tooth structures (Fig. 4T,U). A dental lamina was present in *K14-Cre43*; *Bmpr1a*$^{cl/cl}$ embryos at E13.5, and tooth bud formation was initiated. However, the tooth buds were significantly smaller and less well developed in mutant embryos than in controls (Fig. 4P,Q), and by E16.5 molar and incisor tooth structures had regressed (Fig. 4R,S and data not shown), indicating failure of tooth development after the bud stage.

Epithelial *Bmpr1a* is required for normal postnatal development of hair follicles

At later postnatal stages, dorsal and ventral skin of *K14-Cre52*; *Bmpr1a*$^{cl/cl}$ and *K14-Cre40*; *Bmpr1a*$^{cl/cl}$ mice, and mid-ventral skin of *bcre-32*; *Bmpr1a*$^{cl/null}$ mice, showed striking defects in hair follicle morphology. By P8, control hair follicles were in mid-anagen, with large hair bulbs that had descended deep into the fat layer of the skin, and well-differentiated hair shafts that had undergone terminal differentiation and lacked nuclei. By

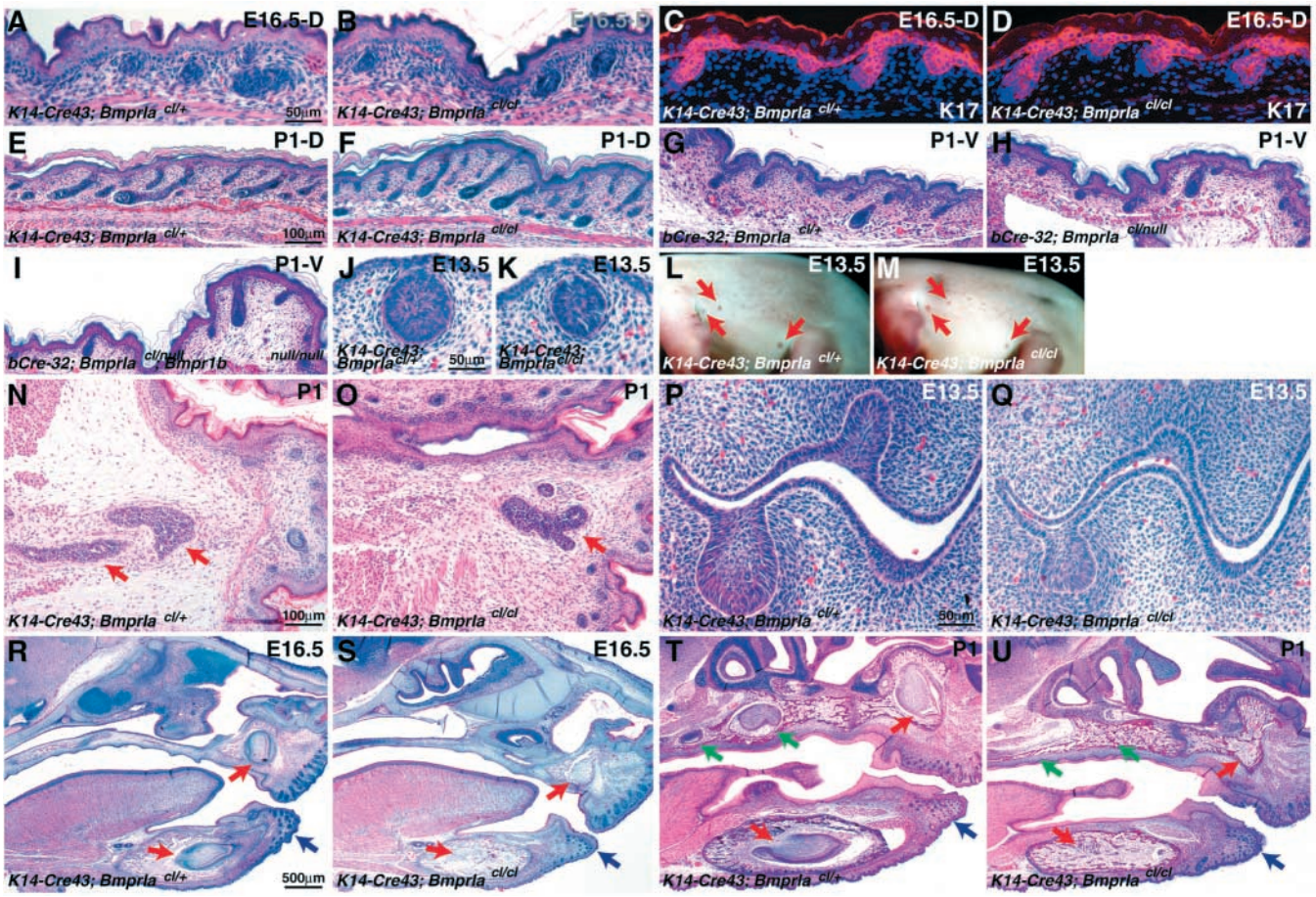

Fig. 4. Embryonic and newborn hair follicle, mammary and tooth phenotypes of mice carrying epidermal-specific deletions of *Bmpr1a*. (A,B) Histology of E16.5 dorsal skin from *K14-Cre43*; *Bmpr1a*$^{cl/+}$ control (A) and *K14-Cre43*; *Bmpr1a*$^{cl/cl}$ (B) embryos. (C,D) Anti-K17 immunofluorescence (red) of skin sections from the embryos shown in A and B, respectively. (E,F) Mid-dorsal skin from *K14-Cre43*; *Bmpr1a*$^{cl/+}$ control (E) and *K14-Cre43*; *Bmpr1a*$^{cl/cl}$ (F) newborns. (G-I) Mid-ventral skin from *bcre-32*; *Bmpr1a*$^{cl/+}$ control (G), *bcre-32*; *Bmpr1a*$^{cl/null}$ (H) and *bcre-32*; *Bmpr1a*$^{cl/null}$; *Bmpr1b*$^{null/null}$ (I) newborns. (J,K) Sagittally sectioned mammary buds from E13.5 *K14-Cre43*; *Bmpr1a*$^{cl/+}$ control (J) and *K14-Cre43*; *Bmpr1a*$^{cl/cl}$ (K) embryos. (L,M) Whole-mount in situ hybridization of E13.5 *K14-Cre43*; *Bmpr1a*$^{cl/+}$ control (L) and *K14-Cre43*; *Bmpr1a*$^{cl/cl}$ (M) embryos with a *Wnt10b* probe. Mammary buds are indicated (arrows). (N,O) Sagittally sectioned inguinal mammary gland (arrows) from newborn *K14-Cre43*; *Bmpr1a*$^{cl/+}$ control (N) and *K14-Cre43*; *Bmpr1a*$^{cl/cl}$ (O) mice. (P,Q) Transverse sections of oral cavity from E13.5 *K14-Cre43*; *Bmpr1a*$^{cl/+}$ control (P) and *K14-Cre43*; *Bmpr1a*$^{cl/cl}$ (Q) embryos showing molar tooth buds. (R,S) Sagittally sectioned E16.5 *K14-Cre43*; *Bmpr1a*$^{cl/+}$ control (R) and *K14-Cre43*; *Bmpr1a*$^{cl/cl}$ (S) heads showing absence of developing incisor teeth in the mutant (red arrows). (T,U) Sagittally sectioned *K14-Cre43*; *Bmpr1a*$^{cl/+}$ control (T) and *K14-Cre43*; *Bmpr1a*$^{cl/cl}$ (U) newborn heads. Incisor teeth (red arrows) and molars (green arrows) are indicated in T and are absent at the corresponding locations in U. Vibrissa follicles (blue arrows) are present in the mutant.

contrast, mutant mice displayed hair follicles that were smaller, and were wavy and misangled. The mutant follicles had not descended as deeply into the dermis as control follicles, and, perhaps in part as a consequence of this, the fat layer appeared less expanded than normal. Reduction of the fat layer probably also resulted from difficulties in feeding caused by tooth defects in some mutants. The hair follicles had misshapen, expanded dermal papillae, and the majority of follicles failed to produce hair shafts. Instead, nuclei were present in the centers of the abnormal follicles (Fig. 5A-D and data not shown).

Bmpr1a is required for BMP pathway activity in postnatal hair follicle epithelium

To determine the effect of Cre-mediated deletion of *Bmpr1a* on activity of the BMP signaling pathway, we used anti-phospho-SMAD1/5/8 antibody to localize phospho-SMADs in *K14-Cre40*; *Bmpr1a*$^{cl/cl}$ skin at P8. We observed greatly reduced staining for phospho-SMAD in the abnormal mutant hair follicle epithelium (Fig. 5E,F). Occasional staining was observed in the suprabasal epidermis, consistent with a report of *Bmpr1b* expression in these cells (Botchkarev et al., 1999). Weak phospho-SMAD staining was present in the dermal papillae of mutant follicles, suggesting that BMP signaling is activated in dermal papillae as an indirect response to lack of epithelial *Bmpr1a*.

Epithelial *Bmpr1a* is required for hair shaft and IRS differentiation

To investigate whether the phenotype of mutant hair follicles

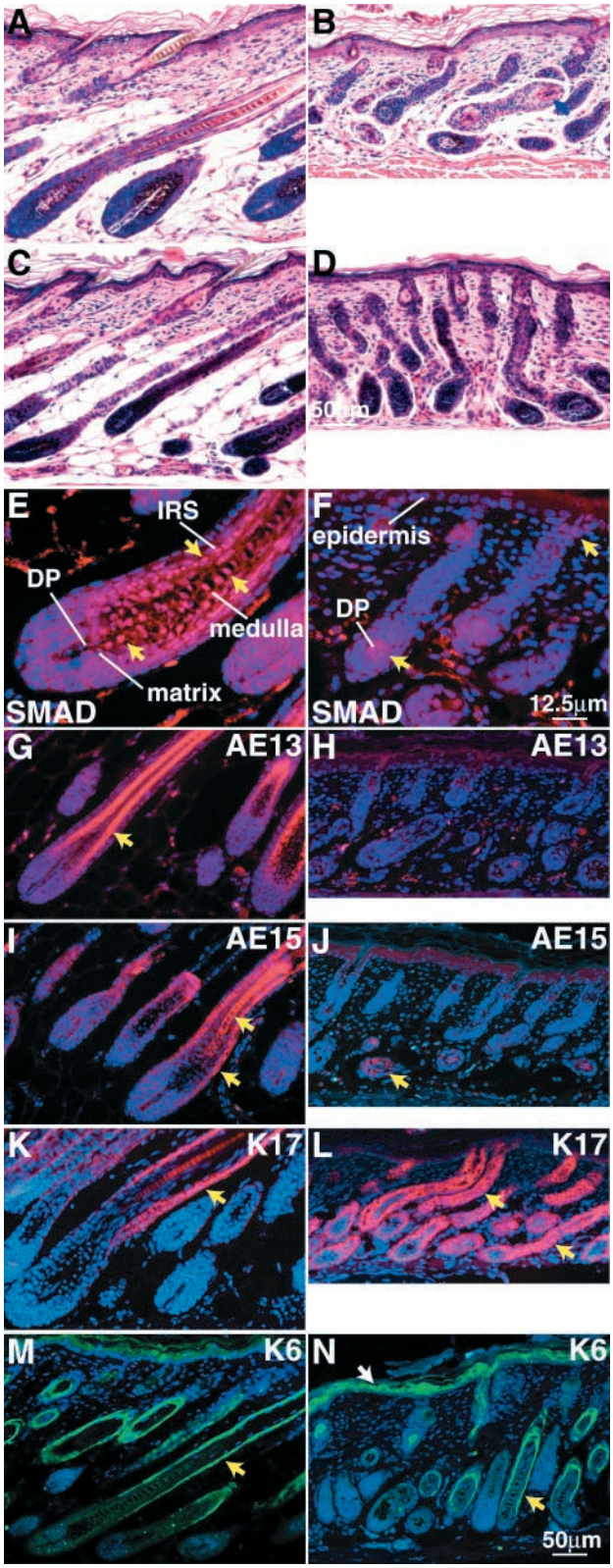

Fig. 5. Effects of epidermal-specific deletion of *Bmpr1a* on the histology of postnatal anagen hair follicles, localization of phospho-SMAD1/5/8, and expression of hair follicle differentiation markers. (A,B) Histology of dorsal skin from *K14-Cre40*; *Bmpr1a*$^{cl/+}$ control littermate (A) and *K14-Cre40*; *Bmpr1a*$^{cl/cl}$ mutant (B) at P8. Nuclei in the center of a mutant follicle are indicated by an arrow (B). (C,D) Histology of mid-ventral skin from *bcre-32*; *Bmpr1a*$^{cl/+}$ control littermate (C) and *bcre-32*; *Bmpr1a*$^{cl/null}$ mutant (D) at P8. (E,F) Anti-phospho-SMAD1/5/8 immmunofluorescence of P8 dorsal skin from *K14-Cre40*; *Bmpr1a*$^{cl/+}$ control littermate (E) and *K14-Cre40*; *Bmpr1a*$^{cl/cl}$ mutant (F). Staining is present in nuclei of IRS and hair-shaft precursors in control follicles (yellow arrows; E) but is much reduced in mutant follicle epithelium (F). Weak staining is present in mutant dermal papillae and in a few epithelial cells close to the epidermis (yellow arrows). (G-L) Immunofluorescence of P8 dorsal skin from *K14-Cre40*; *Bmpr1a*$^{cl/+}$ control littermate (G,I,K) and *K14-Cre40*; *Bmpr1a*$^{cl/cl}$ mutant (H,J,L) using AE13 (G,H), AE15 (I,J) and anti-keratin 17 (K,L) antibodies. (M,N) Immunofluorescence of P8 mid-ventral skin from *bcre-32*; *Bmpr1a*$^{cl/+}$ control littermate (M) and *bcre-32*; *Bmpr1a*$^{cl/null}$ mutant (N) using anti-keratin 6 antibody. Yellow arrows indicate the hair shaft (G), IRS and medulla (I), and outer root sheath (K-N). White arrow indicates epidermal staining (N). Immunofluorescence signals are red in E-L and green in M,N. Nuclei are counterstained with Hoechst 33258. Scale bars: in D applies to A-D; in F applies to E,F; in N applies to G-N.

resulted from abnormal follicular differentiation we examined the expression of several differentiation markers. Staining with AE13, an antibody to type I low-sulfur hair-shaft cortex keratins (Lynch et al., 1986), was absent in the majority of mutant follicles (Fig. 5G,H). Staining with AE15, which recognizes proteins in the medulla of the hair shaft and in the IRS (O'Guin et al., 1992), was greatly reduced in the majority of follicles, and was absent from the most distorted follicles, indicating absence of the hair-shaft medulla and defective differentiation of the IRS (Fig. 5I,J). By contrast, the outer root sheath markers, keratins (K) 17 and 6, were expressed in mutant follicles, and weak K6 expression was observed in mutant epidermis, suggesting epidermal hyperproliferation (Ramirez et al., 1998) (Fig. 5K-N). These results indicated that matrix cells failed to differentiate towards the hair shaft and IRS in mutant follicles, and suggest a crucial role for BMP signaling in hair follicle differentiation.

Transcriptional regulators of IRS and hair-shaft differentiation show reduced or absent expression in mutant follicles

Msx2 function is required for normal expression levels of *Foxn1*, which controls the transcription of several hair keratin genes (Ma et al., 2003; Meier et al., 1999; Schlake and Boehm, 2001). Expression of *Msx2*, the related gene *Msx1*, and *Foxn1* was dramatically reduced in mutant skin (Fig. 6A-D,I,J). Differentiation of the IRS is regulated by the transcription factor GATA3 (Kaufman et al., 2003), and GATA3 expression was similarly reduced or absent in mutant follicles (Fig. 6G,H). Expression of the WNT pathway transcriptional effector *Lef1* was maintained in mutant follicles (Fig. 6K,L); however, nuclear localization of β-catenin, which complexes with LEF1 to activate WNT target transcription, was absent from the epithelium of the most affected follicles (Fig. 6M,N). Nuclear LEF1 and β-catenin localize to hair-shaft precursor cells and are thought to regulate differentiation of the hair shaft (DasGupta and Fuchs, 1999; Merrill et al., 2001). Taken together, therefore, these results indicate that BMPR1A is required for cells exiting the matrix to begin to differentiate to

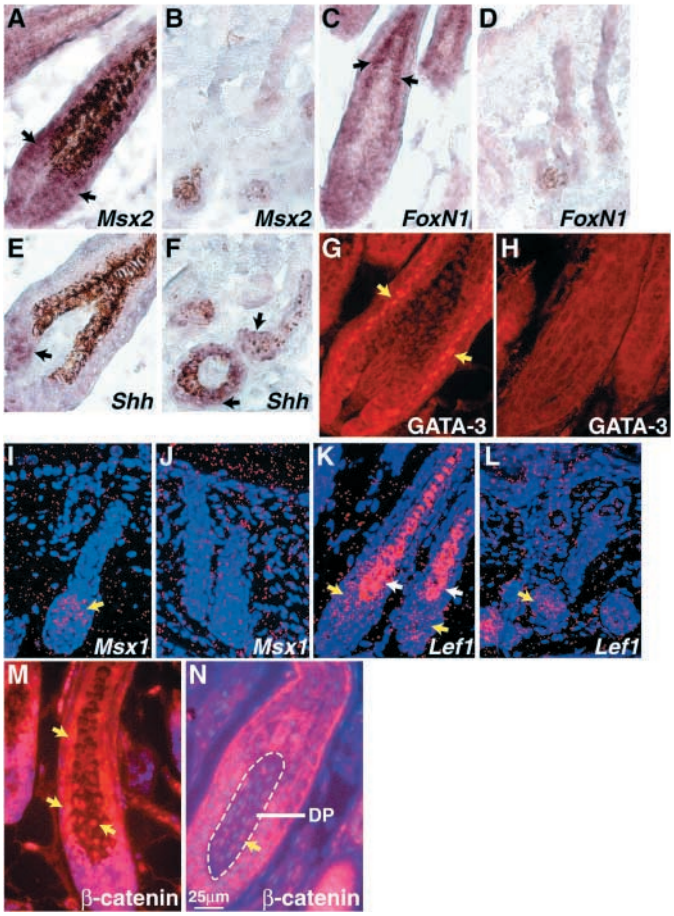

Fig. 6. Effects of epidermal-specific deletion of *Bmpr1a* on expression of regulators of hair shaft and IRS differentiation. (A-F) In situ hybridization of mid-dorsal skin from *K14-Cre40*; *Bmpr1a*$^{cl/+}$ control littermate (A,C,E) and *K14-Cre40*; *Bmpr1a*$^{cl/cl}$ mutant (B,D,F) at P8, using the digoxigenin-labeled antisense probes indicated. Hybridization signals (purple-brown) are indicated by arrows. Dark brown cells (A,E,F) are pigmented. (G,H) Immunofluorescence of P12 dorsal *K14-Cre40*; *Bmpr1a*$^{cl/+}$ control littermate (G) and *K14-Cre40*; *Bmpr1a*$^{cl/cl}$ mutant (H) skin with anti-GATA3. (I,J) In situ hybridization of ventral head skin from *K14-Cre40*; *Bmpr1a*$^{cl/+}$ control littermate (I) and *K14-Cre40*; *Bmpr1a*$^{cl/cl}$ mutant (J) at P8 using ^{35}S-labeled antisense probe for *Msx1*. (K,L) In situ hybridization of mid-ventral P8 skin from *bcre-32*; *Bmpr1a*$^{cl/+}$ control littermate (K) and *bcre-32*; *Bmpr1a*$^{cl/null}$ mutant (L) using ^{35}S-labeled antisense probe for *Lef1*. Bright red regions (K; white arrows) are due to reflection of light by the hair shaft. (M,N) Immunofluorescence for β-catenin (red) in P12 dorsal skin from *K14-Cre40*; *Bmpr1a*$^{cl/+}$ control littermate (M) and *K14-Cre40*; *Bmpr1a*$^{cl/cl}$ mutant (N). Arrows (A,C,E,F,I-L) indicate hybridization signals. Arrows (G,M,N) indicate nuclear localized GATA3 and β-catenin, respectively. Nuclei are counterstained with Hoechst 33258 (I-N). Scale bar in N applies to A-N. DP, dermal papilla.

form hair shaft and IRS. Consistent with this role for BMPR1A, *Shh*, which regulates proliferation in hair follicles (Chiang et al., 1999; Oro and Higgins, 2003; St-Jacques et al., 1998), was expressed in mutant follicles (Fig. 6E,F).

Interestingly, elevated levels of nuclear localized β-catenin were detected in the abnormal, expanded dermal papillae of mutant follicles (Fig. 6N and data not shown). Together with elevated phospho-SMAD1/5/8 in mutant dermal papillae (Fig. 5F), these data suggest that BMP signaling may be capable of activating the WNT pathway in dermal as well as epithelial cells of postnatal follicles.

Mutant hair follicles fail to undergo programmed regression

To determine whether hair follicles cycle normally in the skin of surviving mutant mice, we examined the histology of dorsal and ventral skin from *K14-Cre40*; *Bmpr1a*$^{cl/cl}$ mice at P12, P21 and P34, and ventral skin from *bcre-32*; *Bmpr1a*$^{cl/null}$ mice at P17, compared with control littermates. At P12, control hair follicles were in a fully developed anagen stage, with large hair bulbs and differentiated, pigmented hair shafts (Fig. 7A). Mutant follicles had not descended further into the dermis than they had at P8, and were still wavy and misangled (Fig. 7B). At P17, control follicles were entering catagen (Fig. 7C). By contrast, mutant hair follicles did not regress; instead they persisted in an abnormal anagen phase (Fig. 7D). At P21, control follicles were in the telogen, resting phase, whereas mutant follicles were in an abnormal, anagen-like state (Fig. 7E,F). The dermal papillae of mutant follicles, revealed by staining for alkaline phopshatase, were expanded compared with those of control littermate follicles (Fig. 7E′,F′). Anti-BrdU immunofluorescence revealed high levels of incorporation in the mutant hair follicle bulbs and outer root sheaths at P21 (Fig. 7F″); by contrast, little proliferation was detected in control littermate skin at this stage (Fig. 7E″). By P34, control follicles had re-entered anagen and high levels of proliferation were detected in the follicle bulbs (Fig. 7G,G′). At this stage some less distorted mutant follicles were entering catagen. However, the majority of mutant follicles had still not undergone regression, and cells in the hair bulb and outer root sheath continued to proliferate (Fig. 7H,H′). The mutant epidermis also showed more proliferation than controls (Fig. 7G′,H′). TUNEL assays did not reveal differences in apoptosis between mutant and control anagen stage follicles (not shown).

Long term consequences of epithelial *Bmpr1a* deficiency: development of matricomas and follicular cysts

To assess the longer term consequences of loss of epithelial *Bmpr1a* on the skin we made use of *K14-Cre-ER*^{T2}; *Bmpr1a*$^{cl/cl}$ mice that fortuitously displayed a mild, progressive phenotype due to leakiness of uninduced epidermal Cre-ER^{T2}. This presumably caused a low level of continuous recombination of the *Bmpr1a*^{cl} allele in the basal epidermis and hair follicle stem cells, leading to progressive accumulation of cells that lacked functional BMPR1A (Vasioukhin et al., 1999). At 5 months of age, most control hair follicles were in telogen (not shown). By contrast, skin from *K14-Cre-ER*^{T2}; *Bmpr1a*$^{cl/cl}$ mice and surviving *K14-Cre40*; *Bmpr1a*$^{cl/cl}$ mice contained distorted wavy hair follicles maintained in an abnormal proliferative anagen-like state. In addition, large numbers of benign proliferations that appeared to derive from hair follicles were present, as well as follicular cysts containing dead cells, and, in some cases, massive accumulations of pigment (Fig. 8A,B,D-F, and data not shown). Pigment was extruded to the epidermis via pigmented casts resulting in the appearance of pigment depositions on the skin surface (Fig. 3H,I). Tamoxifen

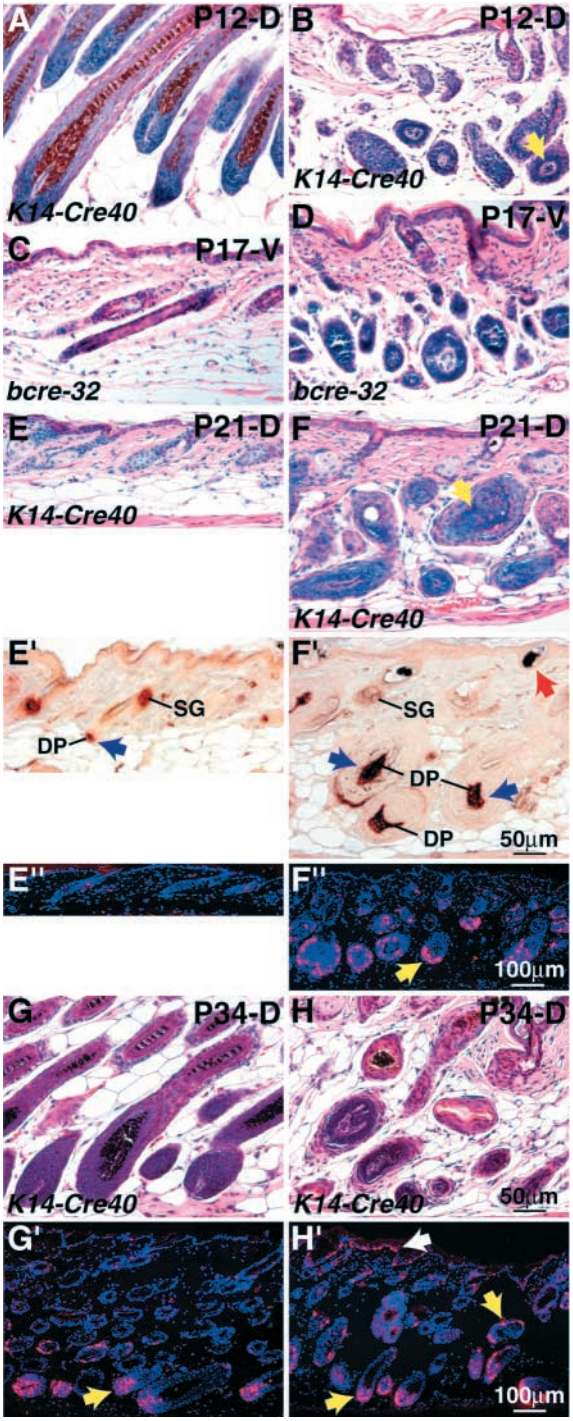

Fig. 7. Abnormal follicular cycling and proliferation in epithelial *Bmpr1a* mutants. (A-F,G,H) Histology of dorsal skin from *K14-Cre40*; *Bmpr1a*$^{cl/+}$ control littermates (A,E,G) and *K14-Cre40*; *Bmpr1a*$^{cl/cl}$ mutants (B,F,H), and ventral skin from *bcre-32*; *Bmpr1a*$^{cl/+}$ control littermate (C) and *bcre-32*; *Bmpr1a*$^{cl/null}$ mutant (D) at P12 (A,B), P17 (C,D), P21 (E,F) and P34 (G,H). Control skin progresses through anagen (A), catagen (C), telogen (E) and first postnatal anagen (G), but mutant skin remains in an abnormal anagen-like state. Arrow in B indicates misshapen, expanded dermal papilla; arrow in F indicates abnormal, undifferentiated cells in the center of a mutant follicle. (E′,F′) Alkaline phosphatase staining of skin sections from the samples shown in E and F, revealing locations of dermal papillae (DP; blue arrows). Red arrow (F′) indicates a pigmented cast being extruded to the epidermis. (E″,F″) Anti-BrdU staining of skin sections from the samples shown in E and F, revealing continued proliferation of mutant follicles (arrow in F″). (G′,H′) Anti-BrdU staining of sections from the samples shown in G and H, showing proliferation in the bulbs of control anagen follicles (G′; yellow arrow), and in the bulbs and outer root sheaths (yellow arrows), and epidermis (white arrow) of mutant skin (H′). Scale bars: in F′ applies to A-F′; in F″ applies to E″,F″; in H applies to G,H; in H′ applies to G′,H′. SG, sebaceous gland.

treatment, to induce higher levels of activity of Cre-ER^{T2}, caused accelerated formation of follicular cysts (Fig. 8C).

To further characterize the abnormal hair follicles, cysts and benign proliferations, we examined their patterns of BrdU incorporation and keratin gene expression. High levels of proliferation were observed in the outer layer of abnormal follicle epithelium, in cyst walls, and in the outer layer of follicle-derived proliferations (Fig. 8G-I). The upper regions of abnormal follicles and the cysts expressed K14, K17 and K6, characteristic of hair follicle outer root sheaths, but did not express the epidermal differentiation marker K1, indicating that they did not differentiate towards epidermis (Fig. 8J,K,M,N,P,Q,S,T). The lower portions of the abnormal follicles and the benign follicular epithelial proliferations did not express keratins, except for very low levels of K17 (Fig. 8J,L,M,O,P,R,S,U). The lack of follicular differentiation within these epithelial proliferations, together with the absence of epithelial nuclear β-catenin (data not shown), suggested that these tumors comprised undifferentiated matrix cells. Follicular tumors comprising such cells are histologically similar to human matricomas rather than pilomatricomas, which typically exhibit prominent hair shaft-like differentiation (Ackerman et al., 2000; Chan et al., 1999). Nuclear phospho-SMADs 1/5/8 were not detected in the dermis surrounding control follicles (not shown), but were present at high levels in the condensed dermis surrounding the proliferations (Fig. 8V), indicating activation of BMP signaling in the dermis. This observation is consistent with previous descriptions of a negative-feedback loop that regulates BMP activity in hair follicles (Botchkarev et al., 2002; Kulessa et al., 2000). A thickened epithelium, unusual expansion of the mesenchyme, and abnormal growth of cartilage and bone were observed under the nails of these mice (Fig. 8W,X), suggesting that loss of BMPR1A from nail epithelium may also induce elevated BMP signaling in the mesenchyme.

Discussion

We show that Cre-mediated loss of epithelial *Bmpr1a* results in striking defects in postnatal hair follicle differentiation, as well as in an early arrest of tooth morphogenesis. Our results indicate that BMPR1A is required for differentiation of both the hair follicle IRS and the hair shaft, suggesting that it plays an early and key role in facilitating the differentiation of matrix cell derivatives.

We observed accelerated embryonic hair follicle development in *Bmpr1a* mutants, consistent with observations that loss of the BMP inhibitor noggin inhibits hair follicle morphogenesis and with data indicating that BMP signals

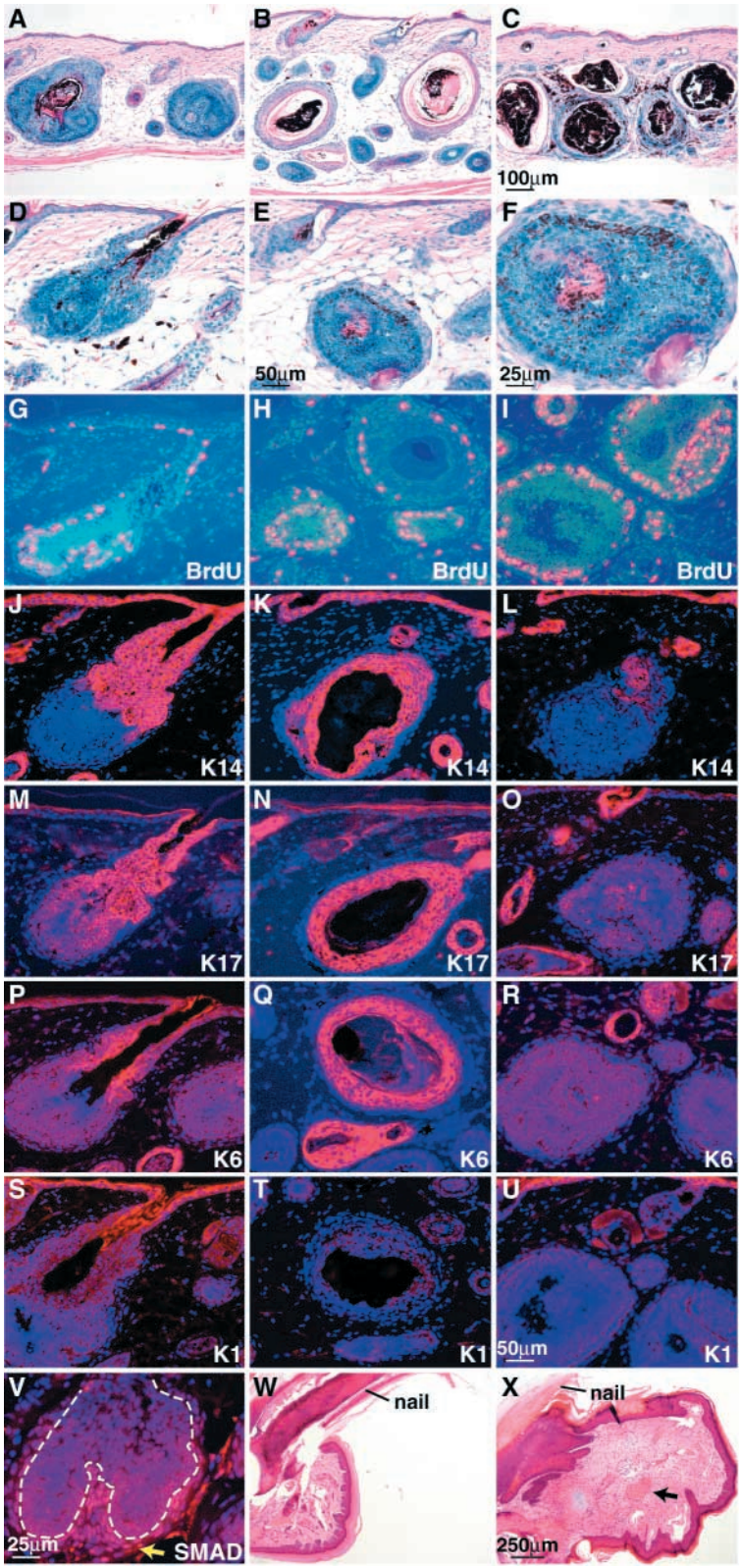

Fig. 8. Development of follicular cysts and matricomas, mesenchymal BMP signaling, and paw phenotype in 5-month-old *K14-Cre-ER^{T2}*; *Bmpr1a$^{cl/cl}$ Bmpr1a* mutant mice. (A-F) Histology of dorsal skin from uninduced (A,B,D-F) and tamoxifen-treated (C) mutants. Abnormal hair follicles are shown in A,D; follicular cysts in B,C; and proliferations of undifferentiated matrix-like cells, histologically similar to human matricomas, in E,F. (G-I) Anti-BrdU immunofluorescence of dorsal skin from uninduced mutants. (J-U) Immunofluorescence of dorsal skin from uninduced mutants with antibodies to the proteins indicated (red). (V) Anti-phospho-SMAD immunofluorescence of abnormal hair follicles showing nuclear phospho-SMAD in dermal cells (arrow). A dashed white line indicates the dermal-epithelial boundary. (W,X) Sagittal sections of the nail region from uninduced control *K14-Cre-ER^{T2}*; *Bmpr1a$^{cl/+}$* mouse (W) and uninduced *K14-Cre-ER^{T2}*; *Bmpr1a$^{cl/cl}$* mutant (X), showing expanded mesenchyme in the mutant. Arrow indicates a calcifying osteoid.

suppress feather follicle fate (Botchkarev et al., 2002; Jung et al., 1998; Noramly and Morgan, 1998). In contrast to this relatively mild embryonic hair follicle phenotype, tooth morphogenesis was highly abnormal in *K14-Cre43*; *Bmpr1a$^{cl/cl}$* mice. A dental lamina was formed, and tooth bud development was initiated; however, at E13.5 these structures were smaller and less developed than in control littermate embryos, and were resorbed by E16.5. These observations are consistent with a previously proposed role for BMP signaling from the mesenchyme to the epithelium that is thought to regulate transition from the bud to the cap stage of tooth development (Jernvall and Thesleff, 2000).

Our finding that deletion of *Bmpr1a* causes severe defects in postnatal differentiation of the hair shaft and IRS is consistent with upregulation of BMP pathway genes during anagen (Botchkarev et al., 2001; Kulessa et al., 2000), and with our observation that nuclear phopsho-SMAD accumulates in hair shaft and IRS precursor cells. Similar defects in hair shaft and IRS differentiation resulting from *K14-Cre*-mediated excision of *Bmpr1a* were reported by Kobielak et al. while this manuscript was under revision (Kobielak et al., 2003), and transgenic mice expressing the BMP inhibitor noggin under the control of an *Msx2* promoter also show defective hair-shaft differentiation (Kulessa et al., 2000). IRS differentiation is relatively normal in *Msx2*-noggin mice, perhaps due in part to the restricted domain of *Msx2* promoter activity and to the fact that noggin downregulates the *Msx2* promoter and so is not expressed at high levels.

In *Bmpr1a* mutant hair follicles, we observe absent or severely decreased expression of the hair-shaft regulatory genes *Foxn1*, *Msx1* and *Msx2*. This suggests that BMPR1A signaling may not activate hair-shaft keratin gene expression directly, but instead by inducing expression of *Msx* genes, which in turn activate *Foxn1* (Ma et al., 2003). In addition, we find that expression of GATA3, a transcription factor that regulates differentiation of matrix cells into IRS (Kaufman et al., 2003), requires epithelial BMPR1A, a result that was also obtained by Kobielak et al. (Kobielak et al., 2003).

Although hair-shaft keratins and several transcription factors associated with terminal differentiation are strongly downregulated or not expressed in *Bmpr1a* mutants, *Lef1*

expression was maintained in the matrix of mutant follicles. Despite expression of *Lef1*, nuclear translocation of β-catenin, indicating activation of the WNT pathway, was not observed in the epithelium of the most affected mutant follicles, suggesting that WNT pathway activation lies downstream of epithelial BMPR1A signaling. The recent identification of *Foxn1* as a direct WNT target gene (Balciunaite et al., 2002) suggests that BMPR1A might regulate *Foxn1* expression by dual mechanisms: activation of WNT signaling and induction of *Msx* expression.

In wild-type hair follicles, matrix cells cease proliferating as they rise up in the follicle beyond the level of the dermal papilla, and begin to express transcription factors that regulate differentiation of the hair shaft and IRS. In the absence of epithelial *Bmpr1a*, post-mitotic cells are observed in the upper follicle bulb (Fig. 7F″,H′; Fig. 8G), but these fail to express regulatory factors or to differentiate towards either hair shaft or IRS. Thus *Bmpr1a* is not required for exit from the highly proliferative matrix compartment, but regulates the next step: differentiation.

Interestingly, the more severely affected epithelial *Bmpr1a*-deficient hair follicles do not undergo programmed regression, but instead continue to proliferate, eventually forming follicular cysts and matricomas. As nuclear localized phospho-SMAD is dramatically decreased at the anagen-catagen transition, it is unlikely that epithelial BMPR1A plays a direct role in initiating catagen onset. Instead, continued proliferation of mutant follicles may indicate that, in the absence of terminal differentiation, the factors that normally signal the end of anagen are not produced. Alternatively, as we find that BMP signaling is active in the hair follicle bulge during the resting phase, and ectopic noggin induces anagen onset (Botchkarev et al., 2001), it is possible that epithelial BMPR1A signaling normally acts to suppress the proliferation of stem cells. Proliferation of these cells in the absence of epithelial BMPR1A could potentially feed expansion of the matrix, over-riding the signals that would normally induce catagen, and, in the absence of follicular differentiation, leading to the development of matricomas.

We thank Richard Behringer for sharing unpublished data; George Cotsarelis and Ed Morrisey for helpful discussions; Elaine Fuchs for the *K14* promoter; Andrew McMahon for the *Shh* plasmid; Pierre Coulombe for anti-K17; Henry Sun for AE13 and AE15 antibodies; Peter ten Dijke for anti-BMPR1A; Philippe Soriano for the *ROSA26R* mice; Dorothy Campbell, Annette Sheldon and Mark Chapman for histology; and Jean Richa for transgenic mouse production. This work was supported by NIH grants AR47709 (S.E.M.), DC03917 and NS39159 (E.B.C.).

References

Ackerman, A. B., Reddy, V. B. and Soyer, H. P. (2000). Neoplasms with follicular differentiation. New York: Ardor Scribendi.

Ahn, K., Mishina, Y., Hanks, M. C., Behringer, R. R. and Crenshaw, E. B., 3rd (2001). BMPR-IA signaling is required for the formation of the apical ectodermal ridge and dorsal-ventral patterning of the limb. *Development* **128**, 4449-4461.

Andl, T., Reddy, S. T., Gaddapara, T. and Millar, S. E. (2002). WNT signals are required for the initiation of hair follicle development. *Dev. Cell* **2**, 643-653.

Balciunaite, G., Keller, M. P., Balciunaite, E., Piali, L., Zuklys, S., Mathieu, Y. D., Gill, J., Boyd, R., Sussman, D. J. and Hollander, G. A. (2002). Wnt glycoproteins regulate the expression of FoxN1, the gene defective in nude mice. *Nat. Immunol.* **3**, 1102-1108.

Botchkarev, V. A. (2003). Bone morphogenetic proteins and their antagonists in skin and hair follicle biology. *J. Invest. Dermatol.* **120**, 36-47.

Botchkarev, V. A., Botchkareva, N. V., Roth, W., Nakamura, M., Chen, L. H., Herzog, W., Lindner, G., McMahon, J. A., Peters, C., Lauster, R. et al. (1999). Noggin is a mesenchymally derived stimulator of hair-follicle induction. *Nat. Cell Biol.* **1**, 158-164.

Botchkarev, V. A., Botchkareva, N. V., Nakamura, M., Huber, O., Funa, K., Lauster, R., Paus, R. and Gilchrest, B. A. (2001). Noggin is required for induction of the hair follicle growth phase in postnatal skin. *FASEB J.* **15**, 2205-2214.

Botchkarev, V. A., Botchkareva, N. V., Sharov, A. A., Funa, K., Huber, O. and Gilchrest, B. A. (2002). Modulation of BMP signaling by noggin is required for induction of the secondary (nontylotrich) hair follicles. *J. Invest. Dermatol.* **118**, 3-10.

Bunting, M., Bernstein, K. E., Greer, J. M., Capecchi, M. R. and Thomas, K. R. (1999). Targeting genes for self-excision in the germ line. *Genes Dev.* **13**, 1524-1528.

Byrne, C., Tainsky, M. and Fuchs, E. (1994). Programming gene expression in developing epidermis. *Development* **120**, 2369-2383.

Chan, E. F., Gat, U., McNiff, J. M. and Fuchs, E. (1999). A common human skin tumour is caused by activating mutations in beta-catenin. *Nat. Genet.* **21**, 410-413.

Chiang, C., Swan, R. Z., Grachtchouk, M., Bolinger, M., Litingtung, Y., Robertson, E. K., Cooper, M. K., Gaffield, W., Westphal, H., Beachy, P. A. et al. (1999). Essential role for Sonic hedgehog during hair follicle morphogenesis. *Dev. Biol.* **205**, 1-9.

Cotsarelis, G., Sun, T. T. and Lavker, R. M. (1990). Label-retaining cells reside in the bulge area of pilosebaceous unit: implications for follicular stem cells, hair cycle, and skin carcinogenesis. *Cell* **61**, 1329-1337.

DasGupta, R. and Fuchs, E. (1999). Multiple roles for activated LEF/TCF transcription complexes during hair follicle development and differentiation. *Development* **126**, 4557-4568.

Dassule, H. R., Lewis, P., Bei, M., Maas, R. and McMahon, A. P. (2000). Sonic hedgehog regulates growth and morphogenesis of the tooth. *Development* **127**, 4775-4785.

Decimo, D., Georges-Labouesse, E. and Dolle, P. (1995). In situ hybridization of nucleic acid probes to cellular RNA. In *Gene Probes Practical Approach Series*, vol. 2 (ed. B. D. Hames and S. J. Higgins), pp. 183-210. Cambridge: IRL Press.

Grachtchouk, V., Grachtchouk, M., Lowe, L., Johnson, T., Wei, L., Wang, A., de Sauvage, F. and Dlugosz, A. A. (2003). The magnitude of hedgehog signaling activity defines skin tumor phenotype. *EMBO J.* **22**, 2741-2751.

Handjiski, B. K., Eichmuller, S., Hofmann, U., Czarnetzki, B. M. and Paus, R. (1994). Alkaline phosphatase activity and localization during the murine hair cycle. *Br. J. Dermatol.* **131**, 303-310.

Hardy, M. H. (1992). The secret life of the hair follicle. *Trends Genet.* **8**, 55-60.

Indra, A. K., Li, M., Brocard, J., Warot, X., Bornert, J. M., Gerard, C., Messaddeq, N., Chambon, P. and Metzger, D. (2000). Targeted somatic mutagenesis in mouse epidermis. *Horm. Res.* **54**, 296-300.

Jernvall, J. and Thesleff, I. (2000). Reiterative signaling and patterning during mammalian tooth morphogenesis. *Mech. Dev.* **92**, 19-29.

Jowett, A. K., Vainio, S., Ferguson, M. W., Sharpe, P. T. and Thesleff, I. (1993). Epithelial-mesenchymal interactions are required for msx1 and msx2 gene expression in the developing murine molar tooth. *Development* **117**, 461-470.

Jung, H. S., Francis-West, P. H., Widelitz, R. B., Jiang, T. X., Ting-Berreth, S., Tickle, C., Wolpert, L. and Chuong, C. M. (1998). Local inhibitory action of BMPs and their relationships with activators in feather formation: implications for periodic patterning. *Dev. Biol.* **196**, 11-23.

Kaufman, C. K., Zhou, P., Pasolli, H. A., Rendl, M., Bolotin, D., Lim, K. C., Dai, X., Alegre, M. L. and Fuchs, E. (2003). GATA-3: an unexpected regulator of cell lineage determination in skin. *Genes Dev.* **17**, 2108-2122.

Kobielak, K., Pasolli, H. A., Alonso, L., Polak, L. and Fuchs, E. (2003). Defining BMP functions in the hair follicle by conditional ablation of BMP receptor IA. *J. Cell Biol.* **163**, 609-623.

Kulessa, H., Turk, G. and Hogan, B. L. (2000). Inhibition of Bmp signaling affects growth and differentiation in the anagen hair follicle. *EMBO J.* **19**, 6664-6674.

Lewandoski, M. (2001). Conditional control of gene expression in the mouse. *Nat. Rev. Genet.* **2**, 743-755.

Li, M., Indra, A. K., Warot, X., Brocard, J., Messaddeq, N., Kato, S.,

Metzger, D. and Chambon, P. (2000). Skin abnormalities generated by temporally controlled RXRalpha mutations in mouse epidermis. *Nature* **407**, 633-636.

Lindner, G., Botchkarev, V. A., Botchkareva, N. V., Ling, G., van der Veen, C. and Paus, R. (1997). Analysis of apoptosis during hair follicle regression (catagen). *Am. J. Pathol.* **151**, 1601-1617.

Lynch, M. H., O'Guin, W. M., Hardy, C., Mak, L. and Sun, T. T. (1986). Acidic and basic hair/nail ("hard") keratins: their colocalization in upper cortical and cuticle cells of the human hair follicle and their relationship to "soft" keratins. *J. Cell Biol.* **103**, 2593-2606.

Ma, L., Liu, J., Wu, T., Plikus, M., Jiang, T. X., Bi, Q., Liu, Y. H., Muller-Rover, S., Peters, H., Sundberg, J. P. et al. (2003). 'Cyclic alopecia' in Msx2 mutants: defects in hair cycling and hair shaft differentiation. *Development* **130**, 379-389.

McGowan, K. M. and Coulombe, P. A. (1998). Onset of keratin 17 expression coincides with the definition of major epithelial lineages during skin development. *J. Cell Biol.* **143**, 469-486.

Meier, N., Dear, T. N. and Boehm, T. (1999). Whn and mHa3 are components of the genetic hierarchy controlling hair follicle differentiation. *Mech. Dev.* **89**, 215-221.

Merrill, B. J., Gat, U., DasGupta, R. and Fuchs, E. (2001). Tcf3 and Lef1 regulate lineage differentiation of multipotent stem cells in skin. *Genes Dev.* **15**, 1688-1705.

Millar, S. E. (2002). Molecular mechanisms regulating hair follicle development. *J. Invest. Dermatol.* **118**, 216-225.

Mishina, Y. (2003). Function of bone morphogenetic protein signaling during mouse development. *Front. Biosci.* **8**, d855-d869.

Mishina, Y., Suzuki, A., Ueno, N. and Behringer, R. R. (1995). Bmpr encodes a type I bone morphogenetic protein receptor that is essential for gastrulation during mouse embryogenesis. *Genes Dev.* **9**, 3027-3037.

Mishina, Y., Hanks, M. C., Miura, S., Tallquist, M. D. and Behringer, R. R. (2002). Generation of Bmpr/Alk3 conditional knockout mice. *Genesis* **32**, 69-72.

Noramly, S. and Morgan, B. A. (1998). BMPs mediate lateral inhibition at successive stages in feather tract development. *Development* **125**, 3775-3787.

O'Guin, W. M., Sun, T. T. and Manabe, M. (1992). Interaction of trichohyalin with intermediate filaments: three immunologically defined stages of trichohyalin maturation. *J. Invest. Dermatol.* **98**, 24-32.

Oliver, R. F. and Jahoda, C. A. (1988). Dermal-epidermal interactions. *Clin. Dermatol.* **6**, 74-82.

Oro, A. E. and Higgins, K. (2003). Hair cycle regulation of Hedgehog signal reception. *Dev. Biol.* **255**, 238-248.

Oshima, H., Rochat, A., Kedzia, C., Kobayashi, K. and Barrandon, Y. (2001). Morphogenesis and renewal of hair follicles from adult multipotent stem cells. *Cell* **104**, 233-245.

Phippard, D. J., Weber-Hall, S. J., Sharpe, P. T., Naylor, M. S., Jayatalake, H., Maas, R., Woo, I., Roberts-Clark, D., Francis-West, P. H., Liu, Y. H. et al. (1996). Regulation of Msx-1, Msx-2, Bmp-2 and Bmp-4 during foetal and postnatal mammary gland development. *Development* **122**, 2729-2737.

Phippard, D., Lu, L., Lee, D., Saunders, J. C. and Crenshaw, E. B., 3rd (1999). Targeted mutagenesis of the POU-domain gene Brn4/Pou3f4 causes developmental defects in the inner ear. *J. Neurosci.* **19**, 5980-5989.

Ramirez, A., Vidal, M., Bravo, A. and Jorcano, J. L. (1998). Analysis of sequences controlling tissue-specific and hyperproliferation-related keratin 6 gene expression in transgenic mice. *DNA Cell Biol.* **17**, 177-185.

Reddy, S., Andl, T., Bagasra, A., Lu, M. M., Epstein, D. J., Morrisey, E. E. and Millar, S. E. (2001). Characterization of Wnt gene expression in developing and postnatal hair follicles and identification of Wnt5a as a target of Sonic hedgehog in hair follicle morphogenesis. *Mech. Dev.* **107**, 69-82.

Schlake, T. and Boehm, T. (2001). Expression domains in the skin of genes affected by the nude mutation and identified by gene expression profiling. *Mech. Dev.* **109**, 419-422.

Soriano, P. (1999). Generalized lacZ expression with the ROSA26 Cre reporter strain. *Nat. Genet.* **21**, 70-71.

St-Jacques, B., Dassule, H. R., Karavanova, I., Botchkarev, V. A., Li, J., Danielian, P. S., McMahon, J. A., Lewis, P. M., Paus, R. and McMahon, A. P. (1998). Sonic hedgehog signaling is essential for hair development. *Curr. Biol.* **8**, 1058-1068.

Taylor, G., Lehrer, M. S., Jensen, P. J., Sun, T. T. and Lavker, R. M. (2000). Involvement of follicular stem cells in forming not only the follicle but also the epidermis. *Cell* **102**, 451-461.

ten Dijke, P., Yamashita, H., Sampath, T. K., Reddi, A. H., Estevez, M., Riddle, D. L., Ichijo, H., Heldin, C. H. and Miyazono, K. (1994). Identification of type I receptors for osteogenic protein-1 and bone morphogenetic protein-4. *J. Biol. Chem.* **269**, 16985-16988.

Vasioukhin, V., Degenstein, L., Wise, B. and Fuchs, E. (1999). The magical touch: genome targeting in epidermal stem cells induced by tamoxifen application to mouse skin. *Proc. Natl. Acad. Sci. USA* **96**, 8551-8556.

Vassar, R. and Fuchs, E. (1991). Transgenic mice provide new insights into the role of TGF-alpha during epidermal development and differentiation. *Genes Dev.* **5**, 714-727.

Vassar, R., Rosenberg, M., Ross, S., Tyner, A. and Fuchs, E. (1989). Tissue-specific and differentiation-specific expression of a human K14 keratin gene in transgenic mice. *Proc. Natl. Acad. Sci. USA* **86**, 1563-1567.

Veltmaat, J. M., Mailleux, A. A., Thiery, J. P. and Bellusci, S. (2003). Mouse embryonic mammogenesis as a model for the molecular regulation of pattern formation. *Differentiation* **71**, 1-17.

von Bubnoff, A. and Cho, K. W. (2001). Intracellular BMP signaling regulation in vertebrates: pathway or network? *Dev. Biol.* **239**, 1-14.

Wang, X., Zinkel, S., Polonsky, K. and Fuchs, E. (1997). Transgenic studies with a keratin promoter-driven growth hormone transgene: prospects for gene therapy. *Proc. Natl. Acad. Sci. USA* **94**, 219-226.

Wilson, C., Cotsarelis, G., Wei, Z. G., Fryer, E., Margolis-Fryer, J., Ostead, M., Tokarek, R., Sun, T. T. and Lavker, R. M. (1994). Cells within the bulge region of mouse hair follicle transiently proliferate during early anagen: heterogeneity and functional differences of various hair cycles. *Differentiation* **55**, 127-136.

Yi, S. E., Daluiski, A., Pederson, R., Rosen, V. and Lyons, K. M. (2000). The type I BMP receptor BMPRIB is required for chondrogenesis in the mouse limb. *Development* **127**, 621-630.

Yi, S. E., LaPolt, P. S., Yoon, B. S., Chen, J. Y., Lu, J. K. and Lyons, K. M. (2001). The type I BMP receptor BmprIB is essential for female reproductive function. *Proc. Natl. Acad. Sci. USA* **98**, 7994-7999.